Journal of Alloys and Compounds 772 (2019) 418–428

Contents lists available at ScienceDirect

Journal of Alloys and Compounds

journal homepage: http://www.elsevier.com/locate/jalcom

Dissimilar joining of carbon/carbon composites to Ti6Al4V using reactive resistance spot welding

Ali Akbar Shokati, Norman Y. Zhou, John Z. Wen*

Mechanical and Mechatronics Engineering Department, University of Waterloo, 200 University Avenue West, Waterloo, ON N2L 3G1, Canada

ARTICLE INFO

Article history:
Received 5 March 2018
Received in revised form
28 August 2018
Accepted 1 September 2018
Available online 5 September 2018

Keywords:
C/C composite
Titanium alloy
Dissimilar joining
Infiltration
Interfacial microstructure
Shear strength

ABSTRACT

A 2D C/C composite with a high porosity (low strength) and a 3D C/C composite with a low porosity (high strength) were investigated for dissimilar joining to Ti6Al4V via reactive spot welding. It was determined that infiltration of melted metal into the composite and formation of a continuous thin TiC layer at the interface of the joints were the dominant joining mechanisms. The 2D C/C composite with a flat surface was successfully joined to Ti6Al4V due to the infiltration of the melted Ti6Al4V into its porous content. On the other hand, it was necessary to drill rectangular grooves onto the surface of the 3D C/C composite to facilitate the infiltration of the melted Ti into the composite, which produced high-strength joints. Surface patterning was determined to be necessary to join the components with mismatching coefficients of thermal expansion. The strength of the 2D C/C composite and Ti6Al4V joints was found to be 7 MPa, while the maximum strength of the groove-patterned 3D C/C composite and Ti6Al4V joints reached 46 MPa.

1. Introduction

C/C composites are well-known, promising materials for high-temperature applications due to a number of desirable properties and their structural advantages, such as a low density, small coefficient of thermal expansion (CTE), high thermal stability, good ablation and thermal shock resistances, and a high strength-to-weight ratio at elevated temperatures [1–6]. These composites have been investigated for their utilization in automotive, aerospace and other industries to manufacture turbine engine components, heat shields, brakes, nozzles, hot press dies, and high temperature furnaces [2,7–13]. One of the most essential requirements for implementing C/C composites at high temperatures is to package or join them to other materials, such as TiAl, copper, and Ti6Al4V [8,14–21]. In many advanced applications, C/C composites must be joined to Ti6Al4V, which is extensively used to construct high-temperature components due to its low density, outstanding mechanical strength, and excellent chemical stability at high temperatures [14,17–19,22]. In recent years, in order to integrate C/C composites to other components, a variety of joining approaches have been developed, such as brazing, adhesive bonding and diffusion bonding [2,9,11,14,22–26]. Joining the C/C composites via brazing and adhesive bonding usually produces joints that cannot withstand a high temperature [2,10,22]. For instance, brazing materials normally have low melting points and experience mechanical instability at high operating temperatures [2,22]. On the other hand, diffusion bonding usually requires a long processing time and a high operating pressure and temperature (up to 1700 °C). It was reported that treatment of C/C composites under such conditions may result in the deterioration of their mechanical and chemical properties [2,22].

To avoid the shortcomings of the aforementioned joining techniques, integrating the C/C composites and metal substrates without employing a low-melting-point braze interlayer is considered preferable. Nevertheless, directly joining a C/C composite to another component via conventional fusion welding techniques is challenging for two reasons: i) the C/C composite does not melt at the welding temperature due to the high melting point of carbon, and ii) a high residual thermal stress is induced at the interface of the joint caused by the different CTE of the joint components. Therefore, the produced joints have a strong tendency to crack along the interface of the joints, which consequently leads to a deterioration and failure of the joints [11,27–30]. It is therefore desirable to develop a new approach that can successfully address these challenges. Among the multiple research efforts on brazing C/C composites, it has been reported that, while the braze alloys

* Corresponding author.
E-mail address: john.wen@uwaterloo.ca (J.Z. Wen).

https://doi.org/10.1016/j.jallcom.2018.09.018
0925-8388/

contain Ti as the reactive element, the reaction between Ti and solid carbon results in a robust bonding between the braze material and the C/C composite [2,10,31–39]. In terms of the residual stress at the interface of the joint, it was suggested that infiltration of the melted metal into the pores of the C/C composite is beneficial for increasing the joining strength via the interlocking mechanism [10,11,28,40,41]. Furthermore, previous studies on the joining of dissimilar materials indicate that the surface patterning techniques, such as surface puncturing and wave patterning, are promising approaches for releasing the thermal residual stress at the joining interface [11,27–30,42–44]. The patterned interface decreases the residual shear stress and induces the compressive normal stress at the interface of the joints. This type of stress field is beneficial for suppressing the interfacial cracks. In addition, the patterned surface causes an enlarging of the joining area and helps interlock the interface of the joints, which are favorable for the mechanical strength of the joints [11,27–30,42–44]. The same approach can be employed for dissimilar joining of the C/C composite to Ti6Al4V using the reactive spot welding technique. The solid-liquid reaction between the melted titanium and solid carbon can form a chemical bond at the interface of the joint, which further increases the joining strength. Lastly, infiltration of the melted metal into the porosity or groove-patterned surface of the C/C composites can form a mechanical occlusion between the joint components, which tightly pins the interface of the joints.

This study introduces a reactive resistance spot welding technique to develop an innovative and user-friendly method for dissimilar joining of C/C composites to Ti6Al4V. Ti powder was used as the interlayer, whose melting temperature of 1668 °C is comparable to the melting point of Ti6Al4V (1604–1660 °C). This process has been found to be incredibly feasible, cost-effective, very fast (in the millisecond range), and easy to scale up for industrial mass production. In the case of joining the 2D C/C composite, the feasibility of directly joining the flat surface of the 2D C/C composite to Ti6Al4V was investigated. Regarding the joining of the 3D C/C composite and Ti6Al4V, rectangular grooves were machined on the surface of the 3D C/C composite to facilitate the infiltration of the melted Ti into the 3D C/C composite. The effects of the dimensions of the rectangular grooves on the joining strength and fracturing modes of the joints were elucidated.

2. Experiment

The two different C/C composites used in this study were an inexpensive 2D woven C/C composite with a high porosity content (low strength) and a comparatively expensive 3D C/C composite with a low porosity content (high strength). The 2D woven composite was a laminate with a thickness of 2 mm (6 laminas) and an interlaminar shear strength of 8 MPa (provided by Cera Materials). It had a density of 1.51 g/cm^3 and an open porosity content of 14.8%, which resulted from a polymer infiltration and pyrolysis (PIP) process. The 3D C/C composite had a thickness of 5 mm and a density of 1.86 g/cm^3 (provided by HTMAGROUP) and an open porosity content of 4.1%. This high-strength 3D C/C composite was densified via a combination of chemical vapor infiltration (CVI) and resin impregnation process. These C/C composite panels were cut into 25 mm × 30 mm slices for microstructural analysis and 50 mm × 30 mm slices for shear strength testing. The 1 mm thick Ti6Al4V sheets were cut into 25 mm × 30 mm pieces for the microstructural analysis and shear strength testing.

To join with the 2D C/C composite, the melted metal was expected to be infiltrated into its high-porosity content. Moreover, our primary experiments showed that the surface patterning on the 2D C/C composite caused the formation of significant cracks and a deterioration of its mechanical properties. Thus, a flat-surface 2D C/C composite was directly joined to Ti6Al4V. For the 3D C/C composites with a low porosity content, the melted metal was not expected to be infiltrated into its low porosity content. It was therefore necessary to drill a number of rectangular grooves on its surface to facilitate the infiltration of the melted Ti into these grooves. The fabricated grooves were filled with the Ti powder interlayer (purity > 99%, particle size < 44 μm). During joining process, the Ti powder embedded in the grooves was expected to form Ti dentations, which would produce a mechanical interlocking between the joining components. Our study on the effects of the grooves dimensions on the joining strength determined the width of the grooves to range from 0.7 to 1 mm and the depth to range from 1 to 3 mm. The schematic of the groove-patterned 3D C/C composite is presented in Fig. 1(a).

Prior to the joining process, the surfaces were ground to 600 grit using silicon carbide paper and were ultrasonically cleaned in acetone for 30 min. The joining task was conducted using a DC spot welding machine. The flat copper welding electrodes were RWMA Class II, with a diameter of 16 mm. The C/C composite and Ti6Al4V were held in place between two flat electrodes which were used to apply a DC welding current as well as the clamping force during the joining process. The clamping force was set at 2 kN, and a single 200 ms current pulse was used for the weld cycle for all experiments. The hold time was 5 s, and the cooling water flow rate was 4 L/min. The welding current for joining the 2D C/C composite varied from 4 kA to 8 kA in order to investigate the effects of the current on the strength of the joints. For welding currents lower than 4 kA, Joule heating was not sufficient to make a bonding between the joint components. When the current was set to 8 kA, Joule heating was excessive and caused a sticking of the 2D C/C composite surfaces to the copper electrodes. For the 3D C/C composite, its resistance was lower than the 2D C/C composite as a result of a low porosity content of the 3D C/C composite. Therefore, a higher current was necessary to produce adequate Joule heating in order to manufacture a joint. A current of 12 kA was the optimized welding current according to previous experiments. Hence, the current of the joints for the case of joining 3D C/C composite was fixed at 12 kA, and the effects of the rectangular groove dimension on the joining strength were investigated. A schematic diagram of the joining assembly is shown in Fig. 1(b).

The cross-sections of the joints and fracture surfaces were investigated via an optical microscope and scanning electron microscope (SEM) equipped with an energy-dispersive X-ray spectroscopy detector (EDS). In addition, grazing incidence X-ray diffraction (GIXRD) was utilized to identify the chemical composition at the joining interface. Single-lap compressive shear strength tests of the welds were then performed with a universal testing machine at a constant cross head speed of 0.5 mm/min, and five replicates of shear tests were conducted for each joining condition. A schematic of the single-lap compressive shear test setup is provided in Fig. 1(c). The lap shear strength of the joints was calculated as the ratio of the maximum force to the area of the joint surface. The area of the joint was considered to be the area where the C/C composite stuck on the Ti6Al4V side and was measured by ImageJ software.

3. Results and discussion

3.1. Characterization of the microstructures before and after joining

Fig. 2 depicts the surface microstructures of the 2D and 3D C/C composites. Minor cracks and less porosities were observed on the surface of the 3D C/C composite (Fig. 2(b)), while a higher content of macro cracks and porosities were observed on the surface of the 2D C/C composite (Fig. 2(a)). Fig. 3(a–d) shows the SEM

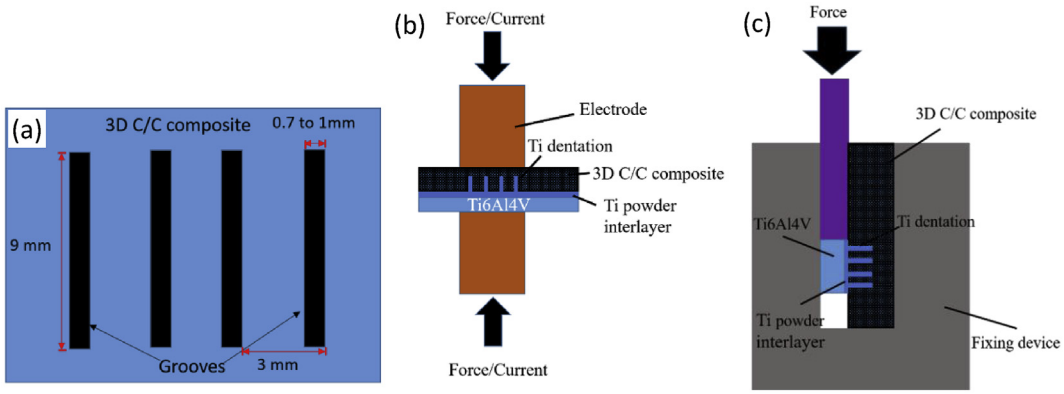

Fig. 1. Schematic of (a) the top view of the fabricated rectangular groove-pattern on the surface of the 3D C/C composite, (b) the setup for joining the groove-patterned 3D C/C composite to Ti6Al4V, and (c) the single-lap compressive shear test setup.

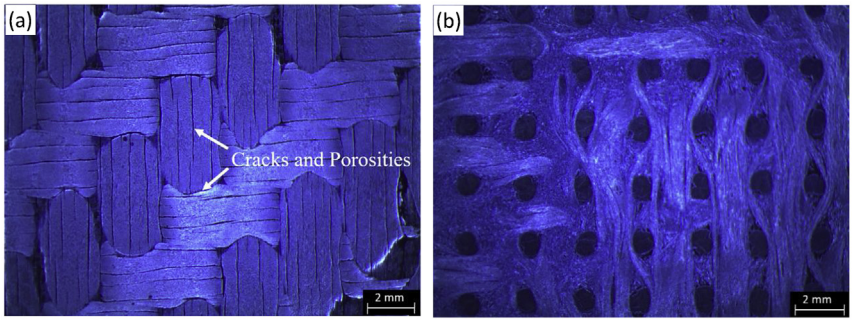

Fig. 2. Optical images of the surface of (a) the 2D C/C composite and (b) the 3D C/C composite.

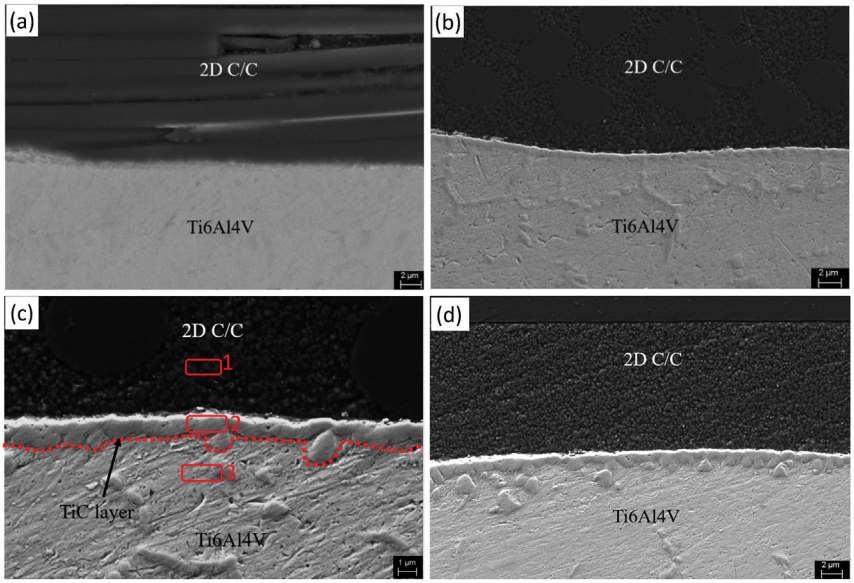

Fig. 3. (a) The interface between the 2D C/C composite and Ti6Al4V for a welding current of 4 kA, (b) 5 kA, (c) 6 kA and (d) 8 kA. EDS analysis was performed on areas of 1, 2 and 3 in (c), as described in the text.

microstructure of the produced Ti6Al4V-2D C/C composite joints with welding currents of 4, 5, 6 and 8 kA, respectively. It was observed that with these applied currents, the interfaces between the Ti6Al4V and 2D C/C composite were microstructurally sound and were free of any major interfacial defects, such as micro voids, pores, and cracks. It can be determined from Fig. 4 that the melted Ti6Al4V infiltrated the pores and cracks existing in the as-delivered 2D C/C composite. The high open porosity content of this composite (14.8%) indeed facilitated the infiltration of the melted Ti6Al4V into its inner structure by a capillary effect [11,45–47]. This process is typical and preferable as it increases the contact area between the composite and Ti6Al4V, which subsequently improves the joining

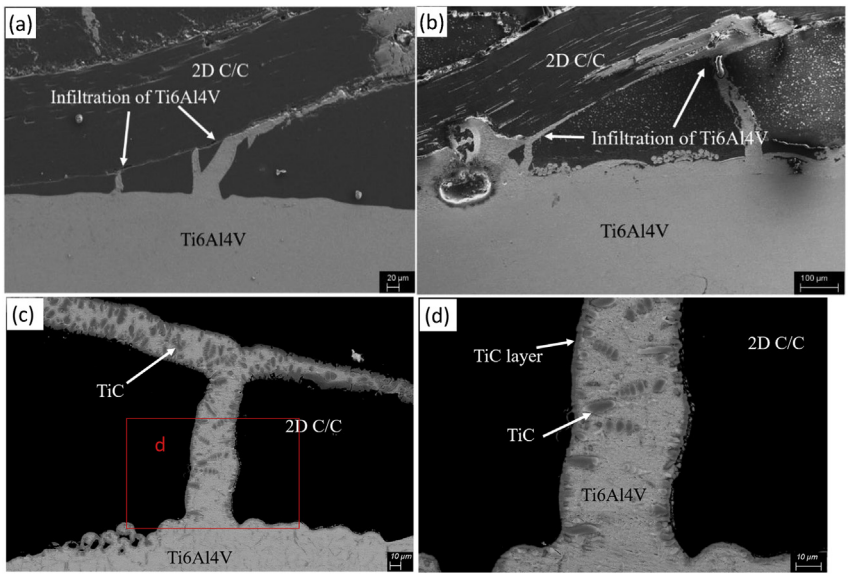

Fig. 4. Typical images showing the penetration and infiltration of the melted Ti6Al4V into the pores and cracks of the 2D C/C composite for a welding current of (a) 5 kA and (b) 6 kA. (c): SEM-backscattered image for 6 kA and (d): zoom-in image of the selected area in (c).

quality. It was suggested in the literature that such an infiltrated structure helps form a mechanical occlusion between the joint components, which tightly pins up the interface of the joint and consequently contributes to the enhanced joining strength [10,11,28,40,41].

Fig. 5 shows the interface of direct joining (without using the Ti powder interlayer) between the flat surface 3D C/C composite and Ti6Al4V. It can be clearly observed that a large number of micro-cracks formed at the joining interface (Fig. 5(a)) as well as within the composite (Fig. 5(b)). A formation of similar cracks was reported by others when dissimilar joining of the flat surface C/C composites to metals was performed [27,30]. It is believed that these cracks are commonly formed as the result of high interfacial residual stresses from the joining process and caused by different CTEs of the joint components [11,27–30]. Moreover, unlike the case of joining the 2D C/C composite, no infiltration of the melted Ti6Al4V into the porosity of the 3D C/C composite was observed due to the low porosity content (4.1%) of the latter. It was found in this study that with the flat 3D C/C composite and Ti6Al4V, the interlocking mechanism was not valid and extra processing was required to improve the joining quality.

To prevent the formation of interfacial cracks and facilitate the infiltration of the melted phase into the 3D C/C composite, a number of rectangular grooves were machined on the surface of the 3D C/C composite and were filled with Ti powder. Fig. 6 shows a typical cross section of the 3D C/C composite-Ti6Al4V joint with a rectangular groove-patterned interfacial structure. As shown in Fig. 6 and later in Fig. 7(a), after the joining process all these rectangular grooves were completely filled with the melted Ti interlayer. The SEM micrographs of the joint between Ti6Al4V and the groove-patterned 3D C/C composite are presented in Fig. 7. Even though minor disconnected microcracks formed at the top of the Ti

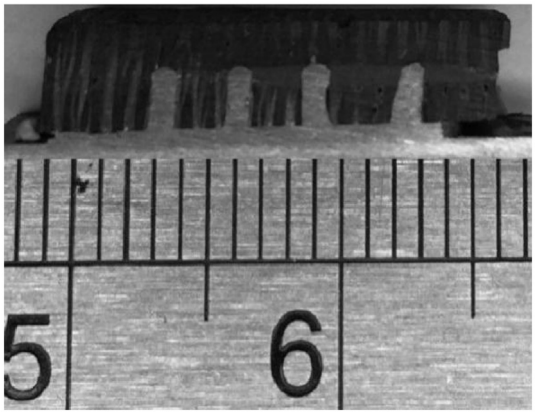

Fig. 6. The cross section of the joint between the rectangular groove-patterned 3D C/C composite and Ti6Al4V.

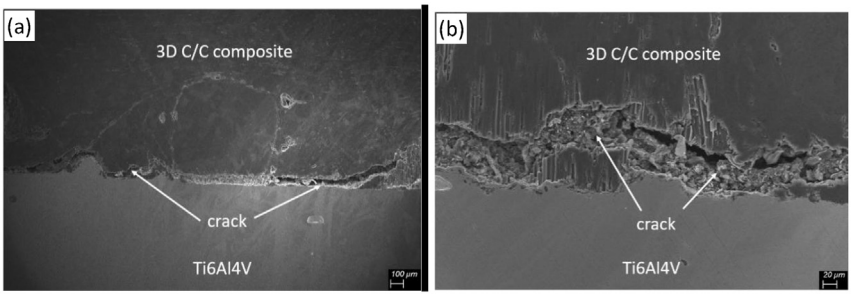

Fig. 5. The interface of the joints between the flat surface 3D C/C composite and Ti6Al4V with two different imaging resolutions.

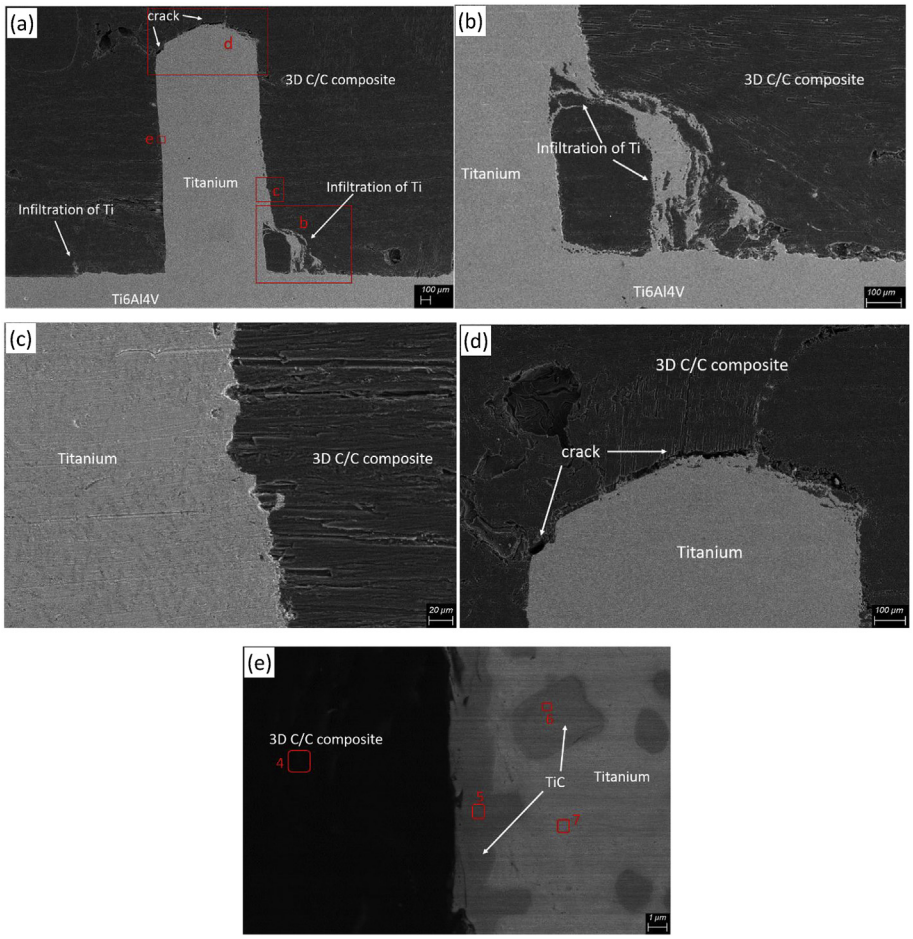

Fig. 7. SEM images of the cross section of the joint between the 3D C/C composite and Ti6Al4V with the groove width of 1 mm and depth of 3 mm: (a) the panorama of the joint interface, where (b), (c), (d) and (e) are zoomed-in images of the selected area in (a).

dentation (shown in Fig. 7(d)), the major region of the joint interface exhibited intimate bonding and was free of structural defects, such as cracks and voids. A comparison between Figs. 5 and 7 clearly demonstrates that adding the rectangular grooves on the 3D C/C composite significantly reduced the interfacial defects. Moreover, infiltration of the melted Ti into the minor cracks of the 3D C/C composite was observed, which brought about the secondary interlocking effect (Fig. 7(a and b)). In earlier studies on joining of the C/C composite, Al_2O_3 and W to metals [27,42,44], researchers indicated that the groove-patterned interface decreases the residual shear stress, induces a compressive normal stress at the interface of the joints, and prohibits the nucleation or growth of the interfacial cracks. They also suggested that, although the surface patterning decreases the overall residual stress at the interface of the joint, the formation of microcracks at the top of the Ti dentation may be caused by the unevenly distributed local residual stress, and it creates the weakest region there.

A thin layer (TiC) with a thickness of 1–2 μm formed at the interface between the C/C composite and Ti6Al4V (shown in Figs. 3(c) and 4(c, d) and 7(e)). In the SEM-backscattered images (Figs. 4(c and d) and 7(e)), this new phase is represented by a continuous dark gray layer at the interface and some dark gray particles embedded in the light gray Ti matrix. According to the literature, this new interfacial phase can be attributed to the reaction between the C/C composite and Ti element [18,34,35,48], and a similar appearance was reported when the C/C composites were joined using compacted titanium powder or the titanium foil as the interlayer [2,31,32,49]. An EDS analysis was performed in this study to confirm the TiC phase, and the results are shown in Table 1. It was found that the areas corresponding to the dark gray thin layer had particles that were rich in C and Ti, which suggests the formation of TiC from the high chemical affinity between Ti and C. Since the Gibb's free energy of forming TiC was highly negative, the reaction between Ti and the C/C composite at the interface was thermodynamically favorable [36,50,51]. Additional tests in this study using GIXRD on the interface of the Ti6Al4V-2D C/C composite joint, shown in Fig. 8, confirm the existence of three phases, including Ti, carbon, and TiC.

A combination of the microstructure observation and the EDS and GIXRD analysis suggests that two dominant joining mechanisms contributed to metallurgical and mechanical bonding between the C/C composite and Ti6Al4V, namely the solid (C/C composite) and liquid (Ti6Al4V/Ti) reaction and the infiltration of the melted metal into the pores or grooves of the C/C composites. Joule heating was introduced via resistance welding, which melted

Table 1
EDS analysis data from Figs. 3(c) and 7(e).

Point	1	2	3	4	5	6	7
Ti (at %)	1.52	39.93	73.97	0.53	57.01	60.58	90.16
C (at %)	98.36	57.00	11.98	99.47	42.99	39.42	9.84
Al (at %)	0.04	2.33	10.08	–	–	–	–
V (at %)	0.09	0.75	3.96	–	–	–	–

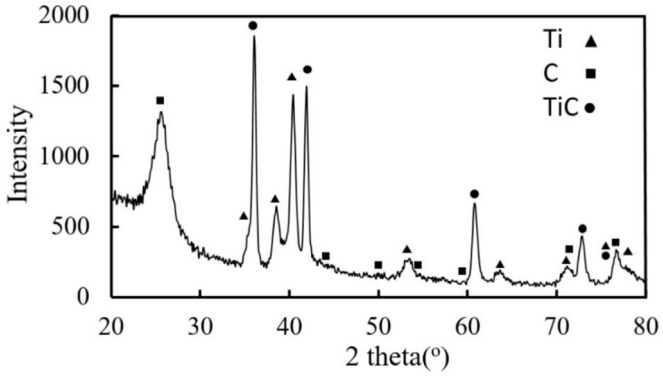

Fig. 8. GIXRD result at the interface of the Ti6Al4V-2D C/C composite joint.

the Ti6Al4V or Ti powder. Subsequently, the reaction between the solid-state C/C composite (due to its high melting point) and the melted metal produced the TiC phase at the interface of the joint. This carbide layer may decrease the interfacial tension and consequently improve the wettability of the molten Ti on the C/C composite [33–37], both leading to an infiltration of the melted metal into the pores and grooves of the composite [33–38].

3.2. Mechanical properties of the joints

Fig. 9(a) shows the lap shear strength of 2D C/C composite-Ti6Al4V joints, which were produced using different welding currents ranging from 4 to 8 kA. The shear strength of these joints remained almost the same (approximately 7 MPa) when the welding current changed from 4 to 6 kA, which is comparable to the maximum interlaminar shear strength of the 2D C/C composite (8 MPa). It should be noted that for all these joining conditions, a fracture occurred within the 2D C/C composite rather than at the interface of the joints (Fig. 10). Therefore, it is reasonable to recommend the reactive resistance spot welding method to join a 2D C/C composite and Ti6Al4V if necessary. However, the bonding strength of such joints was limited by the material strength of the C/C composite, as reported in previous publications [2,28,31,34,36,52–55]. As shown in Fig. 10, the joint failed within the 2D C/C composite, and the line scanning image of the Ti element shows the presence of Ti at the fracture surface, which was the result of an infiltration of melted Ti6Al4V into the 2D C/C composite porosities. As shown in Fig. 9(a), increasing the welding current from 4 to 6 kA resulted in an increased fracture shear force, which was supported by the aforementioned joining mechanisms. By increasing the welding current, Joule heating was increased, and more melted metal was produced, consequently leading to an increased joint area, which contributed to a higher fracture shear force (Fig. 9(a and b)). As seen in Fig. 9(a), the fracture shear force decreased dramatically when increasing the current from 6 to 8 kA. This is explained by the excessive Joule heat produced at the current of 8 kA, which resulted in the 2D C/C composite surface sticking to the copper electrodes. Detachment of the 2D C/C composites from the electrodes caused a damaged 2D C/C surface, as shown in Fig. 11(a and b). Such damage was not observed for the joint processed with the welding current of 6 kA (shown in Fig. 11(c)).

The shear strength values obtained from the joints using the 3D C/C composite with a flat and a groove-patterned interface are presented in Fig. 12. The shear strength of the joints with the flat interface was only 2.34 ± 0.67 MPa. This poor strength of the joint, which was even lower than that from the 2D C/C composite, agrees with the previously described defects and microcracks shown in Fig. 5. In the case of joining the rectangular groove-patterned 3D C/

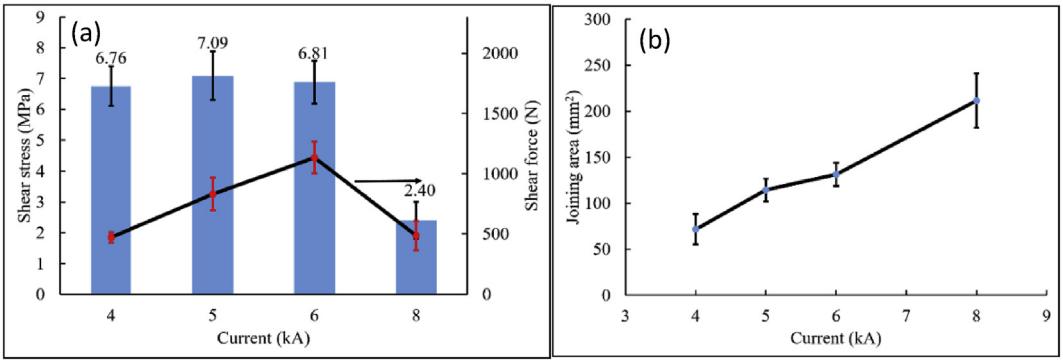

Fig. 9. (a) Shear strength and shear force and (b) joining area of 2D C/C composite-Ti6Al4V joints at different currents.

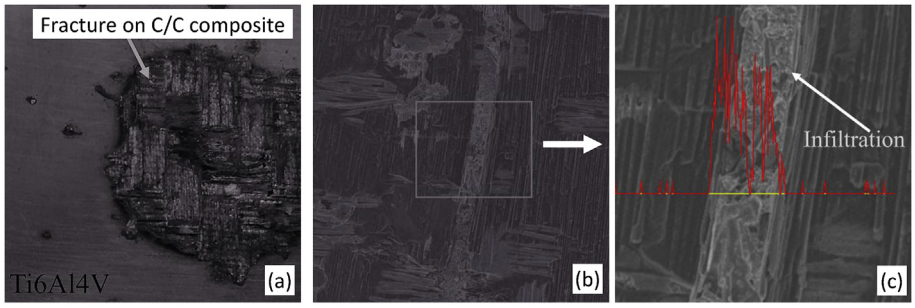

Fig. 10. (a) Typical fractured surface of the 2D C/C composite-Ti6Al4V joint after the shear test, (b) SEM image of the fracture surface and (c) line scanning analysis of the Ti element on the selected area in (b).

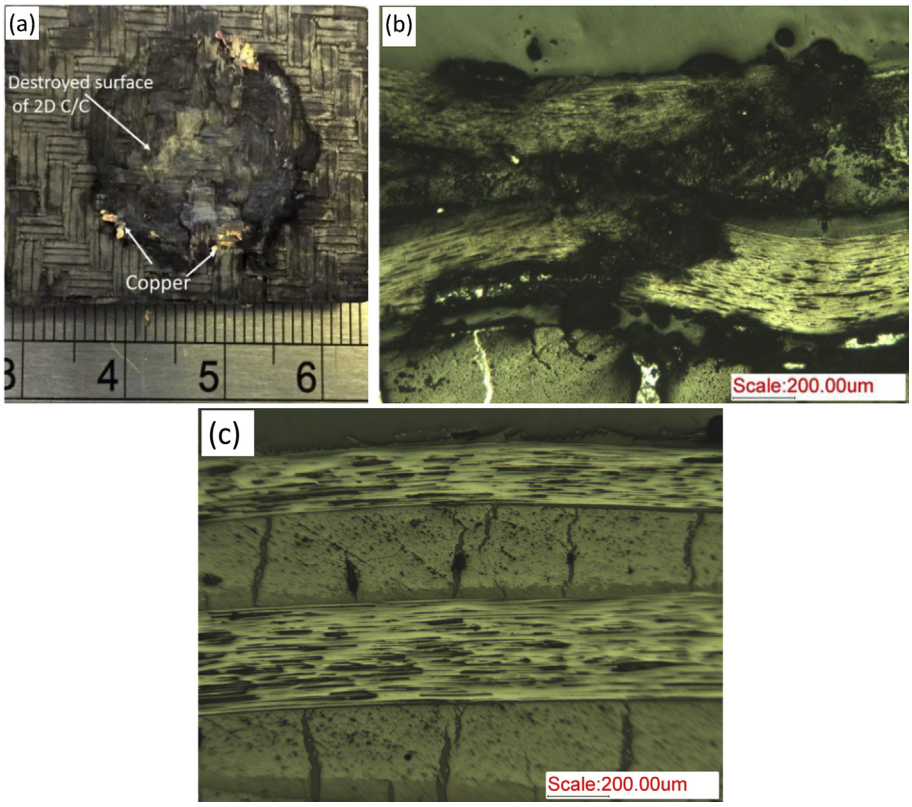

Fig. 11. (a) Photograph of the damaged surface of the 2D C/C composite in contact with the copper electrode for a current of 8 kA, (b) Photograph of the cross section of the joints near the surface of the 2D C/C composite in contact with a copper electrode for a current of 8 kA and (c) 6 kA.

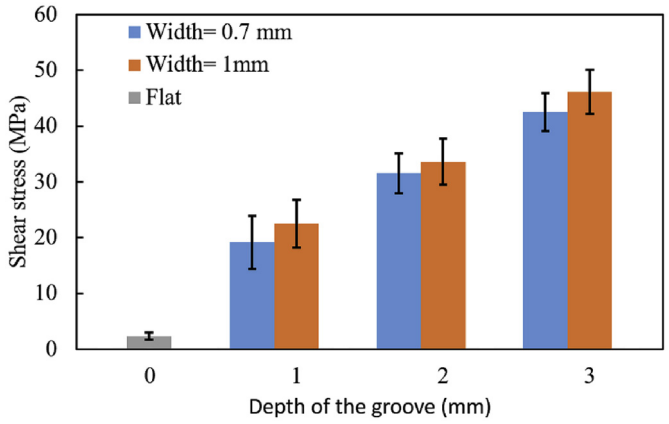

Fig. 12. Shear strength of the 3D C/C composite-Ti6Al4V joints for flat and groove-patterned interfaces with a groove depth between 1 and 3 mm and a width between 0.7 and 1 mm.

C composite, increasing the groove's depth from 1 to 3 mm and the groove's width from 0.7 to 1 mm resulted in a shear strength increase from 19.15 ± 4.81 to 46.14 ± 3.92 MPa, due to the enlarged bonding area. The maximum strength obtained with the groove-patterned interface was significantly higher than that with the flat interface by a factor of approximately 20. This observation confirms that the strength of the joints does not rely only on chemical bonding at the interface but also on the interface patterning. As mentioned earlier, adding the patterned structure decreases the residual stresses as well as induces compressive normal stresses at the interface of the joint, which is beneficial to crack arresting [11,27–30,42–44]. Moreover, embedding the Ti dentations into the rectangular grooves of the 3D C/C pinned the interface of the joint and expanded the joining area, which consequently enhanced the strength of the joints [27–30].

The comparison between the shear strength of the joints using the 2D and 3D C/C composites indicates that the maximum strength of the joints of the 3D C/C composite was 46.14 ± 3.92 MPa, which is approximately 6.5 times higher than the strength obtained from the 2D woven C/C composite (approximately 7 MPa). Note that the shear strength measured on the 2D C/C composite-Ti6Al4V joints in this study is comparable to the values obtained from other investigations [2,9,31,36,52,53]. The shear strength of the 3D C/C composite-Ti6Al4V joints are also comparable to previous studies [7,11,18,19,27,29,41,56,57]. Based on the shear strength measurements, it can be concluded that the C/C-Ti6Al4V joints using the 2D or 3D C/C composites have the potential to be applied in high temperature applications, such as heat shields, nozzles, turbine engines and high temperature furnace components. Moreover, unlike joining the C/C composites via the brazing process, the obtained joints in this study are expected to withstand a high operation temperature due to the exclusion of low melting point braze or filler material during joining. Overall, the 2D C/C composite-Ti6Al4V joints can be used for applications where components are subjected to moderate tensile stresses [31]. By contrast, the 3D C/C composite-Ti6Al4V joint can be used in applications that require high mechanical strength of the joints. In this study, we utilized the groove patterned interface similar to that in the literature to overcome the difficulties of joining dissimilar materials with different coefficients of thermal expansion (i.e., the 3D C/C composite and Ti6Al4V). The investigations on the derived microstructure and mechanical strength of the joints indeed showed that this approach is an effective way to obtain a high-strength joint and can avoid structural defects caused by the different coefficients of

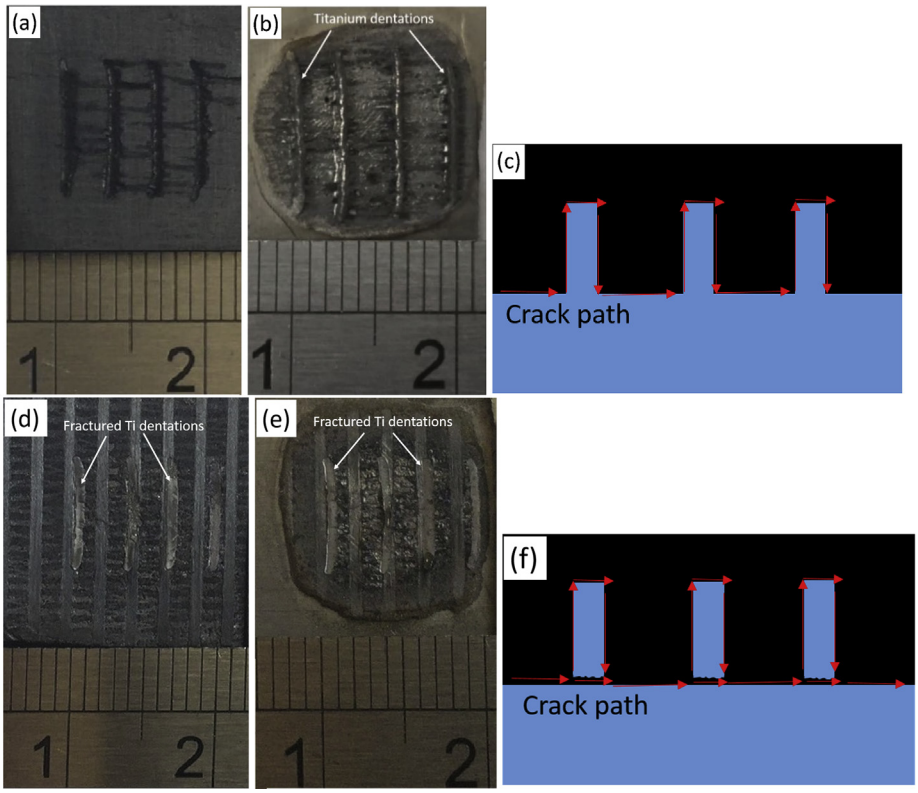

Fig. 13. Typical fractured surfaces on both the 3D C/C composite and Ti6Al4V sides and illustrations of the respective crack propagation path: (a–c) a groove depth of 1 mm and (d–f) a groove depth of 2 and 3 mm.

thermal expansion of the 3D C/C composite and Ti6Al4V.

3.3. *Fracturing modes of joining of the 3D C/C composite to Ti6Al4V*

The dependence of the fracturing mode on the depth of the manufactured grooves may be observed from the macroscopic image of the fractured surface, shown in Fig. 13. For joints with a groove depth of 1 mm, the fracture occurred along the interface between the 3D C/C composite and Ti dentations (Mode 1), whereas for the joints with the groove depth of 2 and 3 mm, the fracture occurred via crack propagation through the infiltrated Ti dentations (Mode 2) (Figs. 13 and 14). The fracturing modes 1 and 2 have been reported previously when dissimilar materials were joined with patterned interfaces [28–30,44,56]. Fig. 13(a–c) shows the fractured surface of the joints with a groove depth of 1 mm. The Ti dentations were completely pulled out from the 3D C/C composite, which revealed the crack propagation at the interface of the joints. The SEM image of the fractured surface of the joints (Fig. 14(a)) shows that the Ti dentations remained intact after the shear test, and no fracture was observed in the infiltrated Ti dentations. The fractured surfaces of the 3D C/C composite joint with a groove depth of 3 mm are shown in Fig. 13(d–f). The Ti dentations were broken and remained on the 3D C/C composite side after the shear test, which indicates that the cracks propagated through the Ti dentations. The SEM images of the fractured surface on the Ti6Al4V side for the joints with groove depths of 3 mm are shown in Fig. 14(d–f), which confirms that fractures occurred in the Ti dentations. The cross-section micrographs of the fractured dentations with depths of 3 mm, after the shear test, are shown in Fig. 15. It shows that the propagation path of the crack existed at the interface and within the 3D C/C composite, agreeing with the combined fracturing mode. It is worthwhile to note that in both modes the crack first initiated at the flat area of the joints and then propagated along the interface. In Mode 1, after the crack reached the Ti dentations, it propagated along the interface between the 3D C/C composite and the Ti dentations, which consequently pulled the Ti dentations out from the 3D C/C composite side. In Mode 2, after the crack reached the Ti dentations, it propagated along two paths. In the first path, some cracks propagated along the interface between the Ti dentations and the 3D C/C composite (Fig. 15). In the second path, some cracks deviated into the Ti dentations and passed through the Ti dentations (Fig. 13(d–f) and Fig. 14(d and e)). Eventually, after reaching the critical load, a fracture occurred within the Ti dentations (Figs. 13(d-f), 14(d, e) and 15). The fracture caused by Mode 2 usually showed a higher shear strength, since more energy was dissipated during the crack propagation in comparison to Mode 1. In Mode 1, the crack propagation was restricted to the interface of the joint between the 3D C/C composite and Ti dentations [56]. Note that in addition to a crack propagation along the interface of the joints, cracks can also be deflected and propagate from the interface of the joints into the 3D C/C composite. It was found that crack deflection is favorable to a change in the fracturing mode from brittle to pseudoplastic, avoiding a catastrophic failure [29,30].

4. Conclusions

In this study, the feasibility of joining C/C composites to Ti6Al4V via the reactive spot welding technique as an innovative joining method for dissimilar materials was investigated and the following conclusions were drawn.

1) It was found that the infiltration of melted Ti/Ti6Al4V plays a key role and is one of the dominant mechanisms of joining the C/C

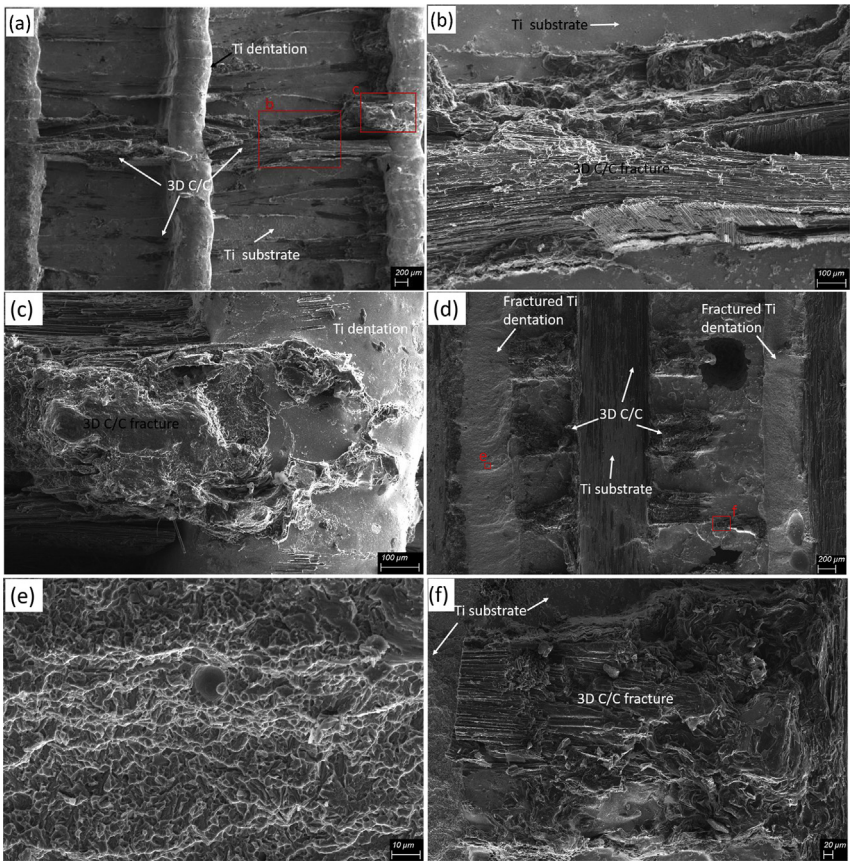

Fig. 14. Typical fracture surfaces of the 3D C/C composite-Ti6Al4V joints on the Ti6Al4V sides for joints with groove depths of (a–c) 1 mm and (d–f) 3 mm.

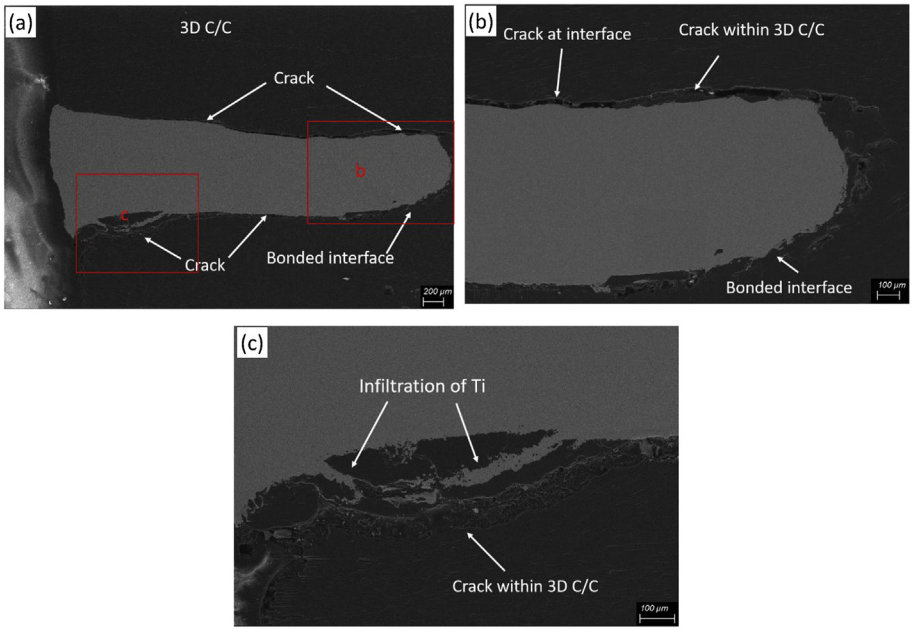

Fig. 15. Cross sections of the microstructure's fractured Ti dentation for the 3D C/C composite-Ti6Al4V joint after a shear test for a groove depth of 3 mm.

composites to Ti6Al4V. A well-bonded joining interface was produced between the 2D C/C composite with a flat surface and Ti6Al4V as the result of the infiltration of the melted Ti6Al4V into the pores of the 2D C/C composite. On the other hand, joining the 3D C/C composite to Ti6Al4V required manufacturing a number of rectangular grooves on the surface of the 3D C/C composite, facilitating the infiltration of the melted Ti into the 3D C/C composite. The groove-patterned interface decreased the

residual stresses and increased the joining area, resulting in a strong interlocking effect, which led to an improved joining strength.

2) The solid-liquid reaction at the interface of the C/C composite-Ti6Al4V joint is another dominant mechanism of joining. Thanks to the Joule heat produced from resistance welding, Ti6Al4V was first melted and then reacted with carbon from the C/C composite, which formed a thin TiC layer with a thickness of 1–2 μm at the interface of the joint. This thin TiC layer improved the mechanical properties of the joints through the formation of chemical bonding at the interface.
3) The 2D C/C composite and Ti6Al4V joints exhibited a maximum strength of approximately 7 MPa, which is close to the interlaminar shear strength of the 2D C/C composite. The groove-patterned 3D C/C composite-Ti6Al4V joints demonstrated a much higher shear strength ranging from 19.15 to 46.14 MPa, due to the formation of interlocked interfacial structures. With the use of Ti powder as the interlayer, which has a melting temperature of 1668 °C (compared to 1604–1660 °C for Ti6Al4V), the developed joining method should be advantageous in high temperature applications.

Data availability

The raw/processed data required to reproduce these findings cannot be shared at this time as the data also form part of an ongoing study (part of the thesis). A permanent link will be provided after the paper is accepted for publication.

Acknowledgement

This work was supported by the Natural Sciences and Engineering Research Council of Canada (NSERC) through a Discovery Grant.

References

[1] X.B. Zhou, H. Yang, F.Y. Chen, Y.H. Han, J. Lee, S.Y. Du, Q. Huang, Joining of carbon fiber reinforced carbon composites with Ti3SiC2 tape film by electric field assisted sintering technique, Carbon 102 (2016) 106–115.
[2] J.D.E. White, A.H. Simpson, A.S. Shteinberg, A.S. Mukasyana, Combustion joining of refractory materials: carbon-carbon composites, J. Mater. Res. 23 (1) (2008) 160–169.
[3] M.C. Wang, X.X. Hu, X.Q. Xu, Z.Q. Yun, J.C. Liu, H.Y. Du, A.R. Guo, A user-friendly heat-resistant modified polymer-based adhesive for joining and repair of carbon/carbon composites, Mater. Des. 86 (2015) 709–713.
[4] Y. Zeng, X. Xiong, G.D. Li, Z.K. Chen, W. Sun, D.N. Wang, Microstructure and ablation behavior of carbon/carbon composites infiltrated with Zr-Ti, Carbon 54 (2013) 300–309.
[5] E. Casal, M. Granda, J. Bermejo, J. Bonhomme, R. Menéndez, Influence of porosity on the apparent interlaminar shear strength of pitch-based unidirectional C–C composites, Carbon 39 (1) (2001) 73–82.
[6] S. Li, X. Chen, Z. Chen, The effect of high temperature heat-treatment on the strength of C/C to C/C–SiC joints, Carbon 48 (11) (2010) 3042–3049.
[7] T.S. Lin, M.X. Yang, P. He, C. Huang, F. Pan, Y.D. Huang, Effect of in situ synthesized TiB whisker on microstructure and mechanical properties of carbon-carbon composite and TiBw/Ti-6Al-4V composite joint, Mater. Des. 32 (8–9) (2011) 4553–4558.
[8] J. Cao, H.Q. Wang, J.L. Qi, X.C. Lin, J.C. Feng, Combustion synthesis of TiAl intermetallics and their simultaneous joining to carbon/carbon composites, Scripta Mater. 65 (3) (2011) 261–264.
[9] M.C. Wang, J.C. Liu, H.Y. Du, F. Hou, A.R. Guo, S. Liu, X. Dong, Joining of C/C composites by using B4C reinforced phosphate adhesive, Ceram. Int. 40 (8) (2014) 11581–11591.
[10] J. Wang, K.Z. Li, X.R. Song, L.J. Guo, W. Li, Z.Q. Li, The study on joining carbon/carbon composites using Ti-Ni-Si compound, Mater. Sci. Eng. A 547 (2012) 12–18.
[11] H.Q. Wang, J. Cao, J.C. Feng, Brazing mechanism and infiltration strengthening of CC composites to TiAl alloys joint, Scripta Mater. 63 (8) (2010) 859–862.
[12] J. Lu, Q. He, Y. Wang, H. Li, Q. Fu, Preparation of co-deposited C/C-ZrC composites by CLVD process and its properties, J. Alloys Compd. 686 (2016) 823–830.
[13] F. Lamouroux, X. Bourrat, R. Naslain, J. Thebault, Silicon carbide infiltration of porous C C composites for improving oxidation resistance, Carbon 33 (4) (1995) 525–535.
[14] W. Guo, L. Wang, Y. Zhu, P.K. Chu, Microstructure and mechanical properties of C/C composite/TC4 joint with inactive AgCu filler metal, Ceram. Int. 41 (5) (2015) 7021–7027.
[15] J. Cao, C. Li, J.L. Qi, Y.L. Shi, J.C. Feng, Combustion joining of carbon-carbon composites to TiAl intermetallics using a Ti-Al-C powder composite interlayer, Compos. Sci. Technol. 115 (2015) 72–79.
[16] J. Zhang, T.P. Wang, C.F. Liu, Y.M. He, Effect of brazing temperature on microstructure and mechanical properties of graphite/copper joints, Mater. Sci. Eng. A 594 (2014) 26–31.
[17] Y.H. Zhou, D. Liu, H.W. Niu, X.G. Song, X.D. Yang, J.C. Feng, Vacuum brazing of C/C composite to TC4 alloy using nano-Al2O3 strengthened AgCuTi composite filler, Mater. Des. 93 (2016) 347–356.
[18] X.R. Song, H.J. Li, V. Casalegno, M. Salvo, M. Ferraris, X.R. Zeng, Microstructure and mechanical properties of C/C composite/Ti6Al4V joints with a Cu/TiCuZrNi composite brazing alloy, Ceram. Int. 42 (5) (2016) 6347–6354.
[19] Y.Q. Qin, Z.S. Yu, Joining of C/C composite to TC4 using SiC particle-reinforced brazing alloy, Mater. Char. 61 (6) (2010) 635–639.
[20] V. Casalegno, M. Salvo, M. Ferraris, Surface modification of carbon/carbon composites to improve their wettability by copper, Carbon 50 (6) (2012) 2296–2306.
[21] X.G. Song, J.H. Chai, S.P. Hu, J. Cao, J.C. Feng, D.Y. Tang, A novel metallization process for soldering graphite to copper at low temperature, J. Alloys Compd. 696 (2017) 1199–1204.
[22] Y.Q. Qin, J.C. Feng, Active brazing carbon/carbon composite to TC4 with Cu and Mo composite interlayers, Mater. Sci. Eng. A 525 (1–2) (2009) 181–185.
[23] M.C. Wang, M.M. Zhuang, X. Tao, X.Q. Xu, H.T. Geng, J.C. Liu, High temperature bonding effect of the room-temperature-curing phosphate adhesive for C/C composites, Key Eng. Mater., Trans Tech Publ (2016) 179–183.
[24] M. Wang, J. Liu, A. Guo, L. Zhao, G. Tian, S. Shen, S. Liu, Preparation and performance of the room-temperature-cured heat-resistant phosphate adhesive for C/C composites bonding, Int. J. Appl. Ceram. Technol. 12 (4) (2015) 837–845.
[25] M. Wang, J. Liu, H. Du, A. Guo, X. Tao, X. Dong, H. Geng, A SiC whisker reinforced high-temperature resistant phosphate adhesive for bonding carbon/carbon composites, J. Alloys Compd. 633 (2015) 145–152.
[26] X. Shi, X. Jin, H. Lin, J. Jing, L. Li, C. Wang, Joining of SiC nanowires-toughened SiC coated C/C composites and nickel based superalloy (GH3044) using Ni71CrSi interlayer, J. Alloys Compd. 693 (2017) 837–842.
[27] J.T. Xiong, J.L. Li, F.S. Zhan, X. Lin, W.D. Huang, Direct joining of 2D carbon/carbon composites to Ti-6Al-4V alloy with a rectangular wave interface, Mater. Sci. Eng. A Struct. Mater. Prop. Microstruct. Process. 488 (1–2) (2008) 205–213.
[28] K.X. Zhang, L.H. Xia, F.Q. Zhang, L.L. He, Active brazing of C/C composite to copper by AgCuTi filler metal, Metall. Mater. Trans. A 47A (5) (2016) 2162–2176.
[29] W. Guo, T. Gao, X. Cui, Y. Zhu, P.K. Chu, Interfacial reactions and zigzag groove strengthening of C/C composite and Rene N5 single crystal brazed joint, Ceram. Int. 41 (9) (2015) 11605–11610.
[30] Y. Shen, Z. Li, C. Hao, J. Zhang, A novel approach to brazing C/C composite to Ni-based superalloy using alumina interlayer, J. Eur. Ceram. Soc. 32 (8) (2012) 1769–1774.
[31] Y.-C. Lin, A.A. Nepapushev, P.J. McGinn, A.S. Rogachev, A.S. Mukasyan, Combustion joining of carbon/carbon composites by a reactive mixture of titanium and mechanically activated nickel/aluminum powders, Ceram. Int. 39 (7) (2013) 7499–7505.
[32] A.S. Mukasyan, J.D.E. White, Combustion joining of refractory materials, Int. J. Self-Propag. High-Temp. Synth. 16 (3) (2007) 154–168.
[33] Y. Qin, J. Feng, Microstructure and mechanical properties of C/C composite/TC4 joint using AgCuTi filler metal, Mater. Sci. Eng., A 454–455 (2007) 322–327.
[34] M. Salvo, V. Casalegno, Y. Vitupier, L. Cornillon, L. Pambaguian, M. Ferraris, Study of joining of carbon/carbon composites for ultra stable structures, J. Eur. Ceram. Soc. 30 (7) (2010) 1751–1759.
[35] D. Liu, Y. Zhou, X. Song, W. Huo, J. Feng, Interfacial microstructure and performance of nano-diamond film/Ti-6Al-4V joint brazed with AgCuTi alloy, Diam. Relat. Mater. 68 (2016) 42–50.
[36] M. Singh, T.P. Shpargel, G.N. Morscher, R. Asthana, Active metal brazing and characterization of brazed joints in titanium to carbon–carbon composites, Mater. Sci. Eng., A 412 (1–2) (2005) 123–128.
[37] M. Singh, R. Asthana, Characterization of brazed joints of CC composite to Cu-clad-Molybdenum, Compos. Sci. Technol. 68 (14) (2008) 3010–3019.
[38] P. Appendino, M. Ferraris, V. Casalegno, M. Salvo, M. Merola, M. Grattarola, Direct joining of CFC to copper, J. Nucl. Mater. 329 (2004) 1563–1566.
[39] F.T. Lan, K.Z. Li, H.J. Li, L.J. Guo, Y.G. He, L.L. Zhang, High-temperature property of carbon/carbon composite joints bonded with ternary Ti-Si-C compound, J. Alloys Compd. 480 (2) (2009) 747–749.
[40] J.T. Xiong, J.L. Li, F.S. Zhang, W.D. Huang, Joining of 3D C/SiC composites to niobium alloy, Scripta Mater. 55 (2) (2006) 151–154.
[41] X.R. Song, H.J. Li, X.R. Zeng, Brazing of C/C composites to Ti6Al4V using multiwall carbon nanotubes reinforced TiCuZrNi brazing alloy, J. Alloys Compd. 664 (2016) 175–180.
[42] J. Li, J.-F. Yang, J.-L. Chen, High heat load properties of actively cooled W/

CuCrZr mock-ups by cladding and diffusion bonding with a two-step process, J. Nucl. Mater. 418 (1) (2011) 110–114.
[43] D. Jiang, J. Long, M. Cai, Y. Lin, P. Fan, H. Zhang, M. Zhong, Femtosecond laser fabricated micro/nano interface structures toward enhanced bonding strength and heat transfer capability of W/Cu joining, Mater. Des. 114 (2017) 185–193.
[44] Y. Zhang, G. Zou, L. Liu, A. Wu, Z. Sun, Y. Zhou, Vacuum brazing of alumina to stainless steel using femtosecond laser patterned periodic surface structure, Mater. Sci. Eng., A 662 (2016) 178–184.
[45] W. Guo, Y. Zhu, L. Wang, P. Qu, H. Kang, P.K. Chu, Microstructure evolution and mechanical properties of vacuum-brazed C/C composite with AgCuTi foil, Mater. Sci. Eng., A 564 (2013) 192–198.
[46] K. Zhang, L. Xia, F. Zhang, L. He, Active brazing of C/C composite to copper by AgCuTi filler metal, Metall. Mater. Trans. 47 (5) (2016) 2162–2176.
[47] J. Wang, K. Li, W. Li, H. Li, Z. Li, L. Guo, The preparation and mechanical properties of carbon/carbon composite joints using Ti–Si–SiC–C filler as interlayer, Mater. Sci. Eng., A 574 (2013) 37–45.
[48] Y.W. Mao, S. Yu, Y.Z. Zhang, B.B. Guo, Z.B. Ma, Q.R. Deng, Microstructure analysis of graphite/Cu joints brazed with (Cu-50TiH(2)) + B composite filler, Fusion Eng. Des. 100 (2015) 152–158.
[49] J.D.E. White, A.S. Mukasyan, M.L. La Forest, A.H. Simpson, Novel apparatus for joining of carbon-carbon composites, Rev. Sci. Instrum. 78 (1) (2007).
[50] M.W. Chase Jr., NIST-JANAF thermochemical tables, J. Phys. Chem. Ref. Data, Monograph 9 (1998), 4th ed.
[51] M. Singh, R. Asthana, Characterization of brazed joints of C-C composite to Cu-clad-Molybdenum, Compos. Sci. Technol. 68 (14) (2008) 3010–3019.
[52] G.N. Morscher, M. Singh, T. Shpargel, R. Asthana, A simple test to determine the effectiveness of different braze compositions for joining Ti-tubes to C/C composite plates, Mater. Sci. Eng. A 418 (1–2) (2006) 19–24.
[53] J.S. Zhang, R.Y. Luo, C.L. Yang, A multi-wall carbon nanotube-reinforced high-temperature resistant adhesive for bonding carbon/carbon composites, Carbon 50 (13) (2012) 4922–4925.
[54] F.T. Lan, K.Z. Li, H.J. Li, Y.G. He, X.T. Shen, W.F. Cao, Joining of carbon/carbon composites for nuclear applications, J. Mater. Sci. 44 (14) (2009) 3747–3750.
[55] V. Casalegno, T. Koppitz, G. Pintsuk, M. Salvo, S. Rizzo, S. Perero, M. Ferraris, Proposal for a modified non-active brazing alloy for joining CFC composites to copper, Compos. Part B Eng. 56 (2014) 882–888.
[56] B. Schedler, T. Huber, T. Friedrich, E. Eidenberger, M. Kapp, C. Scheu, R. Pippan, H. Clemens, Characteristics of an optimized active metal cast joint between copper and C/C, Phys. Scr. 2007 (T128) (2007) 200.
[57] B. Schedler, T. Friedrich, H. Traxler, E. Eidenberger, C. Scheu, H. Clemens, R. Pippan, F. Escourbiac, Examination of C/C flat tile mock-ups with hyper-vapotron cooling after high heat flux testing, Fusion Eng. Des. 82 (3) (2007) 299–305.